10.1562/0031-8655(2000)0720669NLPSOC2.0.CO2

NANOSECOND LASER PHOTOLYSIS STUDIES OF CHLOROSOMES AND ARTIFICIAL AGGREGATES CONTAINING BACTERIOCHLOROPHYLL *e*: EVIDENCE FOR THE PROXIMITY OF CAROTENOIDS AND BACTERIOCHLOROPHYLL *a* IN CHLOROSOMES FROM *Chlorobium phaeobacteroides* strain CL1401

Juan B. Arellano[*†1,2], Thor Bernt Melø[1], Carles M. Borrego[2], Jesús Garcia-Gil[2] and K. Razi Naqvi[1]

[1] Department of Physics, Norwegian University of Science and Technology (NTNU), N–7491, Trondheim, Norway

[2] Laboratory of Microbiology, Institute of Aquatic Ecology, University of Girona, E–17071, Girona, Spain

Key words: Antenna pigments, Bacteriochlorophyll *e*, Carotenoids, Chlorosomes, Isorenieratene, Pigment-pigment interaction, Triplet state.

FOOTNOTES PAGE

*Current address: Instituto de Recursos Naturales y Agrobiología de Salamanca (CSIC), Cordel de Merinas 52, 37008 Salamanca, Spain.

†To whom correspondence should be addressed at: Instituto de Recursos Naturales y Agrobiología de Salamanca (CSIC), Cordel de Merinas 52, 37008 Salamanca, Spain. Fax: +34 923 219609; e-mail: juan@morgat.udg.es

Abbreviations: BChl, bacteriochlorophyll; Car, carotenoid; *Chl.*, *Chlorobium*; *Cfl.*, *Chloroflexus*; 2-HBP, hydroxybiphenyl; Isr, isorenieratene; MGDG, monogalactosyl diglyceride; $\Delta A(\lambda;t)$, time-resolved, laser-induced changes in absorbance; TmS, triplet-minus-singlet.

ABSTRACT

Time-resolved, laser-induced changes in absorbance, $\Delta A(\lambda;t)$, have been recorded with a view to probing pigment-pigment interactions in chlorosomes (control as well as carotenoid-depleted) and artificial aggregates of bacteriochlorophyll *e* (BChl*e*). Control chlorosomes were isolated from *Chlorobium phaeobacteroides* strain CL1401, whose chromophores comprise BChl*e*, bacteriochlorophyll *a* (BChl*a*) and several carotenoid (Car) pigments; Car-depleted chlorosomes, from cells grown in cultures containing 2-hydroxybiphenyl. Artificial aggregates were prepared by dispersing BChl*e* in aqueous phase in the presence of monogalactosyl diglyceride. In chlorosomes $\Delta A(\lambda;t)$ shows, besides a signal attributable to triplet Car (with a half-life of about 4 μs), signals in the Q_y regions of both BChl's. The BChl*a* signal decays at the same rate as the Car signal, which is explained by postulating that some Car's are in intimate contact with some baseplate BChl*a* pigments, and that when a ground-state Car changes into a triplet Car, the absorption spectrum of its BChl*a* neighbours undergoes a concomitant change (termed *transient environment-induced perturbation*). The signal in the Q_y-region of BChl*e* behaves differently: its amplitude falls, under reducing conditions, by more than a factor of two during the first 0.5 μs (a period during which the Car signal suffers negligible diminution), and is much smaller under non-reducing conditions. The BChl*e* signal is also attributed to *transient environment-induced perturbation*, but in this case the perturber is a BChl*e* photoproduct (probably a triplet or a radical ion). The absence of long-lived BChl*e* triplets in all three systems, and of long-lived BChl*a* triplets in chlorosomes, indicates that BChl*e* in densely packed assemblies is less vulnerable to photodamage than monomeric BChl*e* and that, in chlorosome, BChl*a* rather than BChl*e* needs, and receives, photoprotection from an adjacent Car.

INTRODUCTION

Chlorosomes, which function as light harvesters in green photosynthetic bacteria, are oblong bodies attached to the inner side of the cytoplasmic membrane (1, 2). The chlorosomal envelope comprises small proteins, the so-called Csm proteins, and a glycolipid monolayer containing mainly monogalactosyl diglyceride (MGDG); the interior consists of highly aggregated antenna bacteriochlorophyll *x*, (for short BChl*x*, with *x* standing for *c*, *d*, or *e* depending on the species), smaller amounts of monomeric bacteriochlorophyll *a* (BChl*a*), and carotenoid (Car) pigments. The molecular structures of BChl*x* are such that BChl*x*-BChl*x* interactions alone are sufficient for spontaneous aggregation of these pigments; neither a protein scaffold nor the involvement of other chromophores is needed for assembling an artificial, chlorosome-like aggregate (3). Several models for the supramolecular arrangement inside the chlorosomes, envisaging specific interactions, have been put forth (4-6). BChl*a* is thought to form a thin layer on the cytoplasmic membrane side, the so-called baseplate, and has been proposed to be associated to the CsmA protein (7). The baseplate BChl*a* occupies about 1% of the total BChl content in chlorosomes of green photosynthetic bacteria and plays an important role as intermediate in the excitation energy transfer from the chlorosomes to the cytoplasmic membrane-embedded reaction center. Chlorosomes also contain Car's (8,9) in an amount that depends on bacterial species, light conditions, and growth phase (10). The BChl*x*/Car stoichiometric ratio ranges from 3.7/1 to 21/1 in different species of green photosynthetic bacteria (9-11). In addition to the light harvesting pigments, chlorosomes contain quinone (Q) molecules, which could act as quenchers of excitation energy in chlorosomes (12). Traces of oxidised BChl*c* radicals have also been detected, and shown to act as quenchers in native and protein-free reconstituted chlorosomes (13).

Different functions have been suggested for the Car's in chlorosomes. The efficiency of singlet energy transfer from Car to BChl*c* or BChl*e* has been reported to be high in *Chloroflexus* (*Cfl.*) *aurantiacus* (14, 15), *Chlorobium* (*Chl.*) *phaeovibrioides* (16) and *Chl. tepidum* (15), but low in *Chl. phaeobacteroides* (17). It has been suggested that Car's participate in photoprotection by partly quenching the BChl triplet state in chlorosomes (18-20). However, little is known about the precise location of Car pigments within the chlorosomes. There is a proposal (21, 22) that in chlorosomes of *Cfl. aurantiacus*, Car's are in the vicinity of BChl's, and might contribute to the attachment of the chlorosomes to the cytoplasmic membrane *via* the baseplate. Recently, it has been reported (23) that the inhibition of Car biosynthesis, by the addition of 2-hydroxybiphenyl (HBP), affected the BChl*e* Q_y spectral properties, as a consequence of a change in the angle between the transition dipole moment and the rod axis. BChl*a* orientation was not altered, despite a partial loss of this pigment and CsmA protein, suggesting that carotenoids might well play a structural role in maintaining the stability of the chlorosomal baseplate.

The aim of this work is to probe the location of Car chromophores within the chlorosomes of *Chl. phaeobacteroides*, using time-resolved, nanosecond laser kinetic spectroscopy, a technique that has already yielded much useful information on Car-BChl interactions in chlorosomes of *Cfl. aurantiacus* and *Chl. tepidum* (15). By comparing laser-induced changes in the absorbance of control chlorosomes, Car-depleted chlorosomes, and artificial aggregates of BChl*e*, we draw some conclusions concerning the spatial arrangement of chlorosomal pigments. In what follows, the electronic state (ground singlet, lowest triplet, or first excited singlet), of a pigment will be specified by the addition of a superscript (a zero, a dagger, or an asterisk respectively); furthermore, the abbreviation Pyr will denote a chlorophyll (Chl) or a Chl-like pigment.

MATERIALS AND METHODS

Growth conditions and chlorosome isolation. Chl. phaeobacteroides strain CL1401 was grown in standard Pfennig mineral medium (24). Cells were harvested at the beginning of the stationary phase by centrifugation and chlorosomes of *Chl. phaeobacteroides* were isolated on sucrose gradient prepared in 50 m*M* Tris-HCl pH 8.0 and 2 *M* NaSCN (25). A further purification step was carried out using flotation sucrose gradient (26). Inhibition of Car biosynthesis by the addition of HBP and isolation of Car-depleted chlorosomes have been described in a recent publication (23). Chlorosomes were pooled and stored at –80º C.

Artificial aggregates. BChl*e* was purified by HPLC (27). The four main homologues were harvested in one single pool and dried under a stream of nitrogen. The preparation of artificial aggregates was carried out by injecting a 10μl-aliquot of a mixture of BChl*e* and MGDG dissolved in methanol into 3 mL of a vigorously stirred 50 m*M* Tris-HCl pH 8.0 (28). In the assay buffer, MGDG was about 0.003% and the BChl*e* concentration was 12-16 μ*M*, with which absorbance values of 0.6–0.8 were obtained at the BChl*e* Q_y peak. The artificial aggregates were incubated at room temperature for 20 min under an atmosphere of nitrogen in order to reach a steady absorption spectrum before any further measurement.

Absorption spectroscopy. Absorption spectra of chlorosome preparations or artificial aggregates were recorded by using a commercial scanning spectrophotometer (Shimadzu Model UV-160A). The spectral bandwidth of the measuring beam was 2 nm, and the absorbance values were sampled every 1.0 nm.

Nanosecond laser-kinetic spectroscopy. Laser-induced changes in the absorbance of a sample were recorded in the manner described previously (29, 30). Two measurements of the intensity of the monitoring beam after its passage through the sample are needed: one, denoted by $I(\lambda)$, refers to an un-irradiated sample, while the other denoted by $\tilde{I}(\lambda;t)$, is the intensity at time *t* after the sample has been irradiated by a sufficiently short-lived laser pulse. In what follows, the symbols $A(\lambda)$ and $\tilde{A}(\lambda;t)$ will denote the corresponding values of the absorbance, and the optical path length will be denoted by the symbol ℓ. The intensity data were used for calculating the photo-induced change in the absorbance of the sample, $\Delta A(\lambda;t) \equiv \tilde{A}(\lambda;t) - A(\lambda) = \log\left[I(\lambda)/\tilde{I}(\lambda;t)\right]$.

The difference spectra reported here were recorded by means of a multi-channel nanosecond laser flash spectrometer (with a right angle geometry), which has been described earlier in more detail (29). The excitation pulse (with a duration of about 7 ns and an energy of 5-10 mJ) was derived from an optical parametric oscillator pumped by the third harmonic of a Nd:YAG laser. A 250 W xenon arc lamp and a mechanical chopper provided the analyzing beam. A gated optical multichannel analyzer (with a linear dispersion of 0.6 nm per channel) served as the spectrophotometer; with an array of 512 sensing elements (or channels), a single spectrum covers a wavelength interval just over 300 nm wide. For the spectra reported here, the excitation wavelength was tuned to 518 nm, the gate width was held at 20 ns, the delay between the excitation pulse and the opening of the observation window was varied between 100 ns and 5μs, and each time-resolved spectrum represents an average of 2048 spectra. Care was taken to ensure that non-linearities resulting from biphotonic processes could be ignored in the analysis of the spectra reported here.

The concentration of oxygen (an efficient quencher of triplets) was lowered by directing a stream of high-purity argon at the sample surface 10 min prior and during the TmS measurement; the flow of argon was adjusted until it caused a visible depression on the surface without resulting in bubble formation; these conditions are referred to “non-reducing conditions”. “Reducing conditions” were obtained by adding a known aliquot of 1 *M* sodium dithionite to get a final concentration of 15-20 m*M* in the cuvette. After a measurement under reducing conditions, the sodium dithionite absorbance was recorded in the 300-320 nm region to check that the total amount present during the whole experiment remained high enough to maintain reducing conditions.

RESULTS AND DISCUSSION

In the first part of this section absorption spectra of chlorosomes and of artificial aggregates are compared with each other and with previously published absorption spectra of closely related systems; laser-induced changes in these absorption spectra are analyzed in the next subsection.

Absorption spectra

Figure 1 displays $A_a(\lambda)$ and $A_c(\lambda)$, the absorption spectra of artificial aggregates and control chlorosomes, respectively. It is customary to normalize a pair of such spectra at the Q_y peak of BChl*x* (13, 28) even though the wavelengths of the Q_y maxima in the two preparations usually do not coincide; our reason for choosing a different normalization will become apparent shortly. In the case of artificial aggregates of BChl*e*, reproducible results could be obtained only when MGDG was present in the buffer.

In $A_a(\lambda)$, the Q_y band of BChl*e* peaks at 703 nm and the Soret band splits into two bands, one of which peaks at 470 nm, close to the position of the Soret band of monomeric BChl*e* in organic solvents (11), and the other at 527 nm. It is relevant to recall here that the Soret band in *meso,meso*-linked porphyrin arrays (dimer, trimer and tetramer) undergoes a similar splitting (31); the short-wavelength member of the doublet remains coincident with the monomer Soret peak, whereas the long-wavelength member undergoes a redshift which increases with the length of the array.

Control chlorosomes of *Chl. phaeobacteroides* contain BChl*e*, BChl*a* and Car's, mainly isorenieratene (Isr) and β-Isr. The BChl*e*/Car/BChl*a* stoichiometric ratios have been determined to be approximately 100/15/1 (11). In $A_c(\lambda)$, the Q_y peaks of BChl*e* and BChl*a* appear at 716 nm and ~795 nm, respectively. The $S_2 \leftarrow S_0$ absorption band of Car's is buried under the Soret band of BChl*e*, but a judicious normalization, based on our knowledge of the absorption spectra of the Car content of an ethanol extract of control chlorosomes (11), makes it possible to disentangle the bulk of Car contribution from the total absorbance. Assuming the Car absorbance to be negligible for $\lambda \geq 530$ nm, and rather small for $300 \leq \lambda \leq 400$ nm, we normalized the two absorption spectra at 540 nm, thereby bringing $A_c(\lambda)$ and $A_a(\lambda)$ close to each other over the entire 530-650 nm interval as well as in the 300-370 nm interval. The difference, $\Delta_{ca}(\lambda) \equiv A_c(\lambda) - A_a(\lambda)$, is also shown in Fig. 1. The similarity between $\Delta_{ca}(\lambda)$ and the absorption spectrum of the extracted Car's (11) lends confidence to the normalization procedure, and leads one to conclude that the absorbance (in the 300-650 nm region) of BChl*e* in artificial aggregates is close to that in control chlorosomes. On the other hand, the Q_y band in $A_c(\lambda)$ shows a large red shift (13 nm) in relation to that in $A_a(\lambda)$. A comparison of the absorption

spectra of control chlorosomes and Car-depleted chlorosomes shows a similar pattern (23). This means that the splitting of the Soret band (which does not take place in chlorosomes containing BChl*c* or BChl*d*) is a feature common to all three systems examined here.

Laser-induced changes in absorbance

For a system containing a single solute whose molecules are uniformly dispersed at a concentration N, the time-independent, pre-laser absorbance of the sample can be expressed as $A(\lambda) \equiv \varepsilon^0(\lambda) N \ell$, where $\varepsilon^0(\lambda)$ is the extinction coefficient of a ground-state monomer. The post-laser absorbance is contributed by the photoproduct (hereafter assumed to be the triplet) and by the molecules still remaining in the ground state. If $N^\dagger(t)$ and $\varepsilon^\dagger(\lambda)$ denote, respectively, the concentration and the extinction coefficient of the triplets, one has

$$\tilde{A}(\lambda;t) = \varepsilon^\dagger(\lambda) N^\dagger(t) \ell + \varepsilon^0(\lambda)\left[N - N^\dagger(t)\right]\ell \,. \tag{1}$$

The laser-induced change in absorbance can therefore be expressed as

$$\Delta A(\lambda;t) = \left[\varepsilon^\dagger(\lambda) - \varepsilon^0(\lambda)\right] N^\dagger(t) \ell \,. \tag{2}$$

One sees from Eq. (2) that if one is investigating a homogeneous solution, the difference spectrum $\Delta A(\lambda;t) \equiv \tilde{A}(\lambda;t) - A(\lambda)$ will have a positive contribution, made by the photo-generated triplets, and a negative contribution, representing the attendant depopulation of the ground state; hence the name triplet-minus-singlet spectrum. It also follows from Eq. (2) that if one examines a spectral region where neither the parent molecule nor the photoproduct absorbs, that is to say a region where $\varepsilon^0(\lambda) = 0 = \varepsilon^\dagger(\lambda)$, one will have $\Delta A(\lambda) = 0$ throughout this region.

Strictly speaking, the foregoing considerations are seldom applicable to a typical antenna system, where chromophores strongly interact with one another, and the overall absorbance cannot be approximated, except in special cases, by the sum of the absorbances of individual components. The TmS spectra of carotenoids in organic solvents are characterised by an intense positive peak, which is red shifted by about 1000 cm^{-1} with regard to the intensely allowed ($S_2 \leftarrow S_0$) visible band in the ordinary absorption spectrum, and by a few negative peaks in the region of the $S_2 \leftarrow S_0$ band (32). The positive peak arises from $T_n \leftarrow T_1$ transition, and the negative peaks from the loss of Car^0 molecules due to their conversion into $Car^{\dagger}$. These two features are also prominent in the difference spectra of photosynthetic and natural antenna systems (20, 29, 30, 33), and can be unambiguously assigned to the TmS spectrum of antenna Car's. However, the difference spectra of antenna systems also contain a negative signal in the Q_y region, to be denoted by the symbol $\Delta A(Q_y)$, that decays at the same rate as the Car TmS signal. Any $Pyr^{\dagger}$ which does not have a Car^0 neighbor will, of course, contribute a negative peak in the Q_y region, but the lifetime of these "free" Pyr triplets will not coincide with the lifetime of $Car^{\dagger}$. This means that $\Delta A(Q_y)$ cannot be identified with the TmS spectrum of Pyr. Since neither Car^0 nor $Car^{\dagger}$ absorbs in the Q_y region, the presence of $\Delta A(Q_y)$ can be understood only if one concedes that the absorbance of a Pyr^0 which is adjacent to a Car^0 is not identical with that of a Pyr^0 which is adjacent to a $Car^{\dagger}$ (33). Since the change in the absorbance is brought about by a change in the environment of the absorbing entity, and lasts only as long as the labile photoproduct which causes the perturbation, we will refer to this effect as *transient environment-induced perturbation.*

The first step in our investigation of triplet species consisted of recording the laser-induced changes in the absorbance of the simplest system, namely artificial aggregates of

BChl*e*. The aggregates, prepared by using pure BChl*e* and MGDG, should be regarded as artificial aggregates under non-reducing conditions. Figure 2 shows the laser-induced changes (in the 450-800 nm region) in the absorbance of the sample at two delays. The shape of the difference spectrum was found to be independent of the delay time, and the signal decreased by more than a factor of two within 1 μs (data not shown). No significant changes could be seen when the conditions were changed from non-reducing to reducing. The spectrum in Fig. 2, reminiscent of the first derivative of an absorption spectrum, can be easily mimicked by assuming that it is essentially a difference of two spectra, $A(\lambda)$ and $A'(\lambda)$, which have similar shapes but are displaced with respect to each other along the horizontal axis. To illustrate this, $A(\lambda)$ was split into two subspectra, one covering the region $\lambda \leq 600$ nm and the other $\lambda \geq 601$ nm. Each subspectrum was then blue-shifted; the former by 4 nm, and the latter by 1 nm. Finally, a new spectrum, to be denoted by the symbol $A'(\lambda)$, was constructed by merging the two blue-shifted subspectra. Figure 3 shows $A(\lambda)$, $A'(\lambda)$, and $\Delta A_S(\lambda) \equiv A(\lambda) - A'(\lambda)$. The resemblance between, $\Delta A_S(\lambda)$, the simulated difference spectrum and the spectrum plotted in Fig. 2 is sufficiently close to support the view that the latter spectrum is a superposition of $\Delta A_S(\lambda)$ and a second spectrum, with a much smaller amplitude, which is the TmS spectrum of chlorosomal BChl*e* (or the difference spectrum contributed by some other photoproduct). According to this interpretation, the singlet-singlet spectrum of an aggregate of BChl*e* molecules changes, on account of transient environment-induced perturbation, from $A(\lambda)$ to $A'(\lambda)$. The spectra of chlorosomes containing BChl*c* (22) and of the above mentioned *meso*,*meso*-linked porphyrin arrays (31) have been found to display strong electrochromism, and the changes in the absorbance of BChl*e* recorded by us might well be induced by ionic photoproducts; however, the identification of the photoproduct which

causes the perturbation must await further work, particularly the measurement of the Stark spectra of artificial aggregates. At present, we will simply denote the unidentified perturber by the symbol BChl*e*$^{\otimes}$.

Figure 4 shows the difference spectra (in the 510-820 nm range) of control chlorosomes under reducing conditions. The positive peak centered at 535 nm bespeaks the presence of Car triplets. In addition to this, two signals are seen in the Q_y regions of BChl*e* and BChl*a*. Since the former signal is similar to that observed in the difference spectrum of artificial aggregates of BChl*e*, it may be interpreted likewise, and needs no further explanation. As can be seen from Fig. 4, the shape of the difference spectrum $\Delta A(\lambda; t)$ changes with the delay time. During an interval of 0.5 μs, the TmS signal of the Car and the negative peak of BChl*a* showed no perceptible change, but the amplitude of the BChl*e* signal diminished by more than a factor of two. The sub-μs decay of the BChl*e* signal seems to be independent of the presence of Car's and is similar to that observed in artificial aggregates of BChl*e* (Fig. 2) and in Car-depleted chlorosomes under reducing conditions (see Fig. 5). The magnitude of the negative signal in the neighborhood of 795 nm (the Q_y region of BChl*a*) decays in proportion to that of the 535 nm Car peak, and it can therefore be labeled as $\Delta A(Q_y)$ and attributed to Car†-induced perturbation.

The difference spectrum obtained by laser irradiation of Car-depleted chlorosomes of *Chl. phaeobacteroides* under reducing conditions is shown in Fig. 5; essentially the same results were obtained under non-reducing conditions, apart from the fact that the signal in the Q_y region of BChl*e* was much smaller, comparable to that in control chlorosomes under non-reducing conditions (see below). The half-life of the BChl*e*$^{\otimes}$ under reducing conditions (as judged by the rate of decay of the BChl*e*$^{\otimes}$-induced perturbation) was within 1 μs (data not shown); under non-reducing conditions, the signal-to-noise was too low to

allow an estimate of the half-life. The Car peak in Fig. 5 is only four times smaller than that in Fig. 4—despite the fact that the Car-content is now about ten times smaller (23); this behavior parallels that reported for hexane-extracted chlorosomes of *Cfl. aurantiacus* with a Car/BChl*c* ratio ten times smaller than that in control chlorosomes (15). The Car signal is accompanied by the $\Delta A(Q_y)$ band of BChl*a*. The most prominent feature of the difference spectrum in Fig. 5 is the negative signal in the Q_y region of BChl*e*. That it belongs to the TmS spectrum of BChl*e* can be ruled out because, if this were the case, the corresponding negative peak around 525 nm would have been large enough to counterbalance the positive Car TmS contribution. Accordingly, the negative signal should be attributed to perturbation by BChl$e^{\otimes}$, the unidentified transient photoproduct. A comparison of Fig. 5 with Fig. 2 shows that in this case the perturbation amounts more to a decrease in the extinction coefficient of aggregated BChl*e* than an overall shift in the Q_y band. The dissimilarity of the flash-induced changes in the absortion spectra of the three samples investigated here shows that subtle changes in the spatial organization of the pigments can produce substantial changes in the difference spectra arising from transient environment-induced perturbation of the absorption spectrum of aggregated BChl*e*.

The difference spectra of the control chlorosomes under non-reducing conditions at two delays are shown in Fig. 6. The $\Delta A(\lambda;4.5\,\mu s)$ has been multiplied by a factor of 1.9 in order to match $\Delta A(\lambda;0.1\,\mu s)$ at the positive Car peak. Since the overall shape of the difference spectrum (apart from a small region around the BChl*e* Q_y peak) is practically independent of the delay time, we label the negative signal in the region of Q_y peak of BChl*a* as $\Delta A(Q_y)$, and use its presence as an evidence of a strong interaction between Car† and baseplate BChla^0, which implies that some Car pigments are adjacent to some of these BChl*a* molecules. Since monomeric BChl*a* in an organic solvent does show a large

TmS signal (data not shown), since singlet-singlet energy transfer from BChl*e* to BChl*a* does take place (23), and since it does not seem reasonable to postulate that intersystem crossing becomes exceedingly inefficient when the BChl*a* molecules occupy the baseplate, one may infer, from the absence of a TmS signal due to BChl*a* in chlorosomes, that every triplet-forming BChl*a* is contiguous to a Car pigment. If one assumes that all BChl*a* pigments can form triplets, one would be led to conclude that every BChl*a* must be in van der Waals contact with a Car.

In the absence of a signal that can be unambiguously attributed to BChl*e* triplets, we can only discuss various possibilities and their consequences. In the first place, the triplet yield may be too low to give rise to a detectable signal. Secondly, triplet lifetime may be much shorter than 100 ns, the shortest delay used in our studies. Thirdly, the photoproduct which has been labeled BChl$e^{\otimes}$ may in fact be BChl$e^{\dagger}$, which again implies that the triplet lifetime is in the sub-μs range, appreciably shorter than the value (a few hundred μs) noted for the lifetime of monomeric BChl's in organic solvents (34,35). All in all, this reasoning leads one to conclude that BChl*e* does not require any photoprotection. It is most likely that the triplet yield is rather low, due to efficient quenching of chlorosomal BChl*e** (36), and the few triplets which *are* formed undergo rapid migration and are quenched by a ground state molecule, another triplet, or a radical ion (15), and are therefore less susceptible (than a monomeric BChl† which is not adjacent to a quencher) to quenching by molecular oxygen. Using a very sensitive instrument with a newly developed near-infrared sensitive photomultiplier (Hamamatsu R5509-42), we tried but failed to observe singlet oxygen luminescence from our samples (unpublished data). The failure is entirely in keeping with our conclusion concerning the low yield and the short lifetime of BChl*e* triplets in aggregated systems.

It has recently been reported (15) that the height of the Car peak in chlorosomes of *Chl. tepidum* and *Cfl. aurantiacus* does not change when one goes from reducing to non-reducing conditions (whereas the fluorescence yield suffers a noticeable reduction). A comparison of Figs. 4 and 6 shows that the Car $T_n \leftarrow T_1$ peak at 535 nm happens to be about 30% *higher* under non-reducing conditions. Some suggestions have already been advanced to account for the unexpectedly high triplet Car yield in non-reducing conditions (33); here we would like to propose one other possibility. Since these systems contain not only BChl*e* but also Car's and quinones, it is not inconceivable that Car triplets may be produced as a result of charge recombination in a manner analogous to that demonstrated for a Car-Pyr-Fullerene triad (37). Further work is needed to see whether the following mechanism makes any contribution to the production of Car triplets in chlorosomes:

$$\mathrm{Car}^0 - \mathrm{BChl}e^* - \mathrm{Q}^0 \rightarrow \mathrm{Car}^0 - \mathrm{BChl}e^+ - \mathrm{Q}^- \rightarrow \mathrm{Car}^+ - \mathrm{BChl}e^0 - \mathrm{Q}^- \rightarrow \mathrm{Car}^\dagger - \mathrm{BChl}e^0 - \mathrm{Q}^0$$

We conclude by reiterating the main results of this study. The spectra presented above have shown that the lifetime of chlorosomal BChl*e* triplets is so short that formation of singlet oxygen through quenching of these triplet cannot present a serious threat to the chlorosomes, and that Car's are able to protect baseplate BChl*a* monomers.

Acknowledgements. JB Arellano is very grateful to the ESF for awarding him a travel grant for his visit to Trondheim. We also acknowledge financial support from the Research Council of Norway (NFR).

REFERENCES

1. Blankenship, R. E., J. M. Olson and M. Miller (1995) Antenna complexes from green photosynthetic bacteria. In *Anoxygenic Photosynthetic Bacteria* (Edited by R. E. Blankenship, M. T. Madigan and C. E. Bauer), pp. 399–435. Kluwer Academic Publishers, Dordrecht.

2. Olson, J. M. (1998) Chlorosome organization and function in green photosynthetic bacteria. *Photochem. Photobiol.* **67**, 61–75.

3. Holzwarth, A. R., K. Griebenow and K. Schaffner (1990) A photosynthetic antenna system which contains a protein-free chromophore aggregate. *Z. Naturforsch.* **45**, 203–296.

4. Holzwarth, A. R. and K. Schaffner (1994) On the structure of bacteriochlorophyll molecular aggregates in the chlorosomes of green bacteria. A molecular modelling study. *Photosynth. Res.* **41**, 225–233.

5. Mizoguchi, T. K., K. Matsuura, K. Shimada and Y. Koyama (1996) The structure of the aggregate form of bacteriochlorophyll *c* showing the Q_y absorption above 740 nm: a ^{1}H-NMR study. *Chem. Phys. Lett.* **260**, 153–158.

6. Buck, D. R. and W. S. Struve (1996) Tubular exciton models for BChl *c* antennae in chlorosomes from green photosynthetic bacteria. *Photosynth. Res.* **48**, 367–377.

7. Sakuragi, Y., N. U. Frigaard, K. Shimada and K. Matsuura (1999) Association of bacteriochlorophyll *a* with the CsmA protein in chlorosomes of the photosynthetic green filamentous bacterium *Chloroflexus aurantiacus*. *Biochim. Biophys. Acta* **1413**, 172–180.

8. Liaaen-Jensen, S. (1965) Bacterial carotenoids. XVIII. Aryl carotenoids from *Phaeobium*. *Acta Chem. Scand.* **19**, 1025–1030.

9. Schmidt, K. (1980) A comparative study on the composition of chlorosomes (*Chlorobium* vesicles) and cytoplasmic membranes from *Chloroflexus aurantiacus* OK–

70–fl and *Chlorobium limicola* f. *thiosulfatophilum* strain 6230. *Arch. Microbiol.* **124**, 21–31.

10. Oelze, J. and J. R. Golecki (1995) Membranes and chlorosomes of green bacteria: Structure, composition, and development. In *Anoxygenic Photosynthetic Bacteria* (Edited by R. E. Blankenship, M. T. Madigan and C. E. Bauer), pp. 259–278. Kluwer Academic Publishers, Dordrecht.

11. Borrego, C. M., J. B. Arellano, C. A. Abellà, T. Gillbro and L. J. Garcia-Gil (1999) The molar extinction coefficient of bacteriochlorophyll *e* and the pigment stoichiometry in *Chlorobium phaeobacteroides*. *Photosynth. Res.* **60**, 257–264.

12. Frigaard, N. U., S. Takaichi, M. Hirota, K. Shimada and K. Matsuura (1997) Quinones in chlorosomes of green sulfur bacteria and their role in the redox-dependent fluorescence studied in chlorosome-like bacteriochlorophyll *c* aggregates. *Arch. Microbiol.* **167**, 343–349.

13. van Noort, P. I., Y. Zhu, R. LoBrutto and R. E. Blankenship (1997) Redox effects on the excited-state lifetime in chlorosomes and bacteriochlorophyll c oligomers. *Biophys. J.* **72**, 316–325.

14. van Dorssen, R. J., H. Vasmel and J. Amesz (1986) Pigment organization and energy transfer in the green photosynthetic bacterium *Chloroflexus aurantiacus*. II. The chlorosome. *Photosynth. Res.* **9**, 33–45.

15. Melø, T. B., N. U. Frigaard, K. Matsuura and K. R. Naqvi (2000) Electronic energy transfer involving carotenoid pigments in chlorosomes of two green bacteria: *Chlorobium tepidum* and *Chloroflexus auranticus*. *Spectrochim. Acta* Part A. In press.

16. Otte S. C. M., J. C. van der Heiden, N. Pfennig and J. Amesz (1991) A comparative study of the optical characteristics of intact cells of photosynthetic green sulfur bacteria containing bacteriochlorophyll *c*, *d* or *e*. *Photosynth. Res.* **28**, 77–87.

17. Cox, R. P., M. Miller, J. Aschenbrücker, Y. Z. Ma and T. Gillbro (1998) The role of bacteriochlorophyll *e* and carotenoids in light harvesting in brown-colored green sulfur bacteria. In *Photosynthesis*: *Mechanisms and Effects* Vol. 1. (Edited by G. Garab), pp 149–152. Kluwer Academic Publishers, Dordrecht.

18. Psencik, J., G. F. W. Searle, J. Hala and T. J. Schaafsma (1994) Fluorescence detected magnetic resonance (FDMR) of green sulfur photosynthetic bacteria *Chlorobium* sp. *Photosynth. Res*. **40**, 1–10.

19. Psencik, J., T. J. Schaafsma, G. F. W. Searle and J. Hala (1997) Fluorescence detected magnetic resonance of monomers and aggregates of bacteriochlorophylls of green sulfur bacteria *Chlorobium* sp. *Photosynth. Res*. **52**, 83–92.

20. Carbonera, D., G. Giacometti, C. Vannini, P. D. Gerola, A. Vianelli, A. Maniero and L. C. Brunel (1998) Electron magnetic resonance of the chlorosomes from green sulfur bacterium Chlorobium tepidum. In *Photosynthesis*: *Mechanisms and Effects* Vol. 1. (Edited by G. Garab), pp 109–112. Kluwer Academic Publishers, Dordrecht.

21. Foidl, M., J. R. Golecki and J. Oelze (1997) Phototrophic growth and chlorosome formation in *Chloroflexus aurantiacus* under conditions of carotenoid deficiency. *Photosynth. Res.* **54**, 219–226.

22. Frese, R., U. Oberheide, I. van Stokkum, R. van Grondelle, M. Foidl, J. Oelze and H. van Amerongen (1997) The organization of bacteriochlorophyll *c* in *Chloroflexus aurantiacus* and the structural role of carotenoids and protein. *Photosynth. Res.* **54**, 115–126.

23. Arellano, J. B., J. Psencik, C. M. Borrego, Y. Z. Ma, R. Guyoneaud, J. Garcia-Gil and T. Gillbro (2000) Effect of carotenoid biosynthesis inhibition on the chlorosome organization in *Chlorobium phaeobacteroides* strain CL1401. *Photochem. Photobiol.* In press.

24. Trüper, H. G. and N. Pfennig (1992) The family Chlorobiaceae. In *The Prokaryotes. A Handbook on the Biology of Bacteria: Ecophysiology, Isolation, Identification, Applications* (Edited by A. Balows, H. G. Trüper, M. Dworkin, W. Harder and K. H. Schleifer), pp. 3583–3592, 2nd edition. Springer-Verlag, Berlin.

25. Gerola, P. D. and J. M. Olson (1986) A new bacteriochlorophyll *a*-protein complex associated with chlorosomes of green sulfur bacteria. *Biochim. Biophys. Acta* **848**, 69–76.

26. Steensgaard, D. B, K. Matsuura, R. P. Cox and M. Miller (1997) Changes in bacteriochlorophyll *c* organization during acid treatment of chlorosomes from *Chlorobium tepidum*. *Photochem. Photobiol.* **65**, 129–134.

27. Borrego, C. M. and L. J. Garcia-Gil (1994) Separation of bacteriochlorophyll homologues from green photosynthetic sulfur bacteria by reverse-phase HPLC. *Photosynth. Res.* **41**, 157–163.

28. Hirota, M., T. Moriyama, K. Shimada, M. Miller, J. M. Olson and K. Matsuura (1992) High degree of organization of bacteriochlorophyll *c* in chlorosomes-like aggregates spontaneously assembled in aqueous solution. *Biochim. Biophys. Acta* **1099**, 271–274.

29. Naqvi, K. R., T. B. Melø, B. B. Raju, T. Jávorfi, I. Simidjiev and G. Garab (1997) Quenching of chlorophyll *a* singlets and triplets by carotenoids in light-harvesting complex of photosystem II: comparison of aggregates with trimers. *Spectrochim. Acta* Part A **53**, 2659–7667.

30. Büchel, C., K. R. Naqvi and T. B. Melø (1998) Pigment-Pigment interactions in thylakoids and LHCII of chlorophyll *a*/*c* containing alga *Pleurochloris meiringensis*: analysis of fluorescence-excitation and triplet-minus-singlet spectra. *Spectrochim. Acta* Part A **54**, 719–726.

31. Ohta, N., Y. Iwaki, T. Ito, I. Yamazaki and A. Osuka (1999) Photoinduced charged transfer along a *meso,meso*-linked linked porphyrin array. *J. Phys. Chem. B.* **103**, 11242–11245.

32. Jhutti, C. S. (1999) M.Sc. thesis, Norwegian University of Science and Technology.

33. Van der Voss, R., D. Carobonera and A. J. Hoff (1991) Microwave and optical spectroscopy of carotenoid triplets in light-harvesting complex LHCII of spinach by absorbance-detected magnetic resonance. Appl. Magn. Res. **2**, 179–202.

34. Krasnovsky, A. A., P. Cheng, R. E. Blankenship, T. A. Moore and D. Gust (1993) The photophysics of monomeric bacteriochlorophylls *c* and *d* and their derivatives: properties of the triplet state and singlet oxygen photogeneration and quenching. *Photochem. Photobiol.* **57**, 324–330.

35. Krasnovsky, A. A., J. Lopez, P. Cheng, P. A. Liddell, R. E. Blankenship, T. A. Moore and D. Gust (1994) Generation and quenching of singlet molecular oxygen by aggregated bacteriochlorophyll *d* in model systems and chlorosomes. *Photosynth. Res*. **40**, 191–198.

36. Van Walree, C. A., Y. Sakuragi, D. B. Steensgaard, C. S. Bösinger, N.-U. Frigaard, R. P. Cox, A. R. Holzwarth and M. Miller (1999) Effect of alkaline treatment on bacteriochlorophyll *a*, quinones and energy transfer in chlorosomes from *Chlorobium tepidum* and *Chlorobium phaeobacteroides*. *Photochem. Photobiol*. **69**, 322–328.

37. Carbonera, D., M. D. Valentin, C. Corvaja, G. Agostini, G. Giacometti, P. A. Liddell, D. Kuciauskas, A. L. Moore, T. A. Moore and D. Gust (1998) EPR investigation of

photoinduced radical pair formation and decay to a triplet state in carotene-porphyrin-fullerene triad. *J. Am. Chem. Soc.* **120**, 4398–4405.

FIGURE LEGENDS

Figure 1. Absorption spectra, $A_c(\lambda)$ and $A_a(\lambda)$, of (respectively) control chlorosomes and artificial aggregates of BChl*e* in 50 m*M* Tris-HCl pH 8.0. The spectra have been normalized at 540 nm. Also shown is the difference $A_c(\lambda) - A_a(\lambda)$.

Figure 2. Time-resolved, laser-induced changes, $\Delta A(\lambda; t)$, in the absorbance of artificial aggregates of BChl*e* at two delays. The initial absorbance was 0.6 at 703 nm.

Figure 3. Simulation of the difference spectrum plotted in Fig. 2; see the text for an explanation of the symbols and further details.

Figure 4. Time-resolved, laser-induced changes, $\Delta A(\lambda; t)$, in the absorbance of control chlorosomes under reducing conditions (15 m*M* sodium dithionite) at different delays. The initial absorbance was 0.8 at 716 nm. The inverted absorption of chlorosomes is plotted for better comparison.

Figure 5. Time-resolved, laser-induced changes, $\Delta A(\lambda; t)$, of Car-depleted chlorosomes under reducing conditions at two delays. The initial absorbance was 0.8 at 703 nm. The inverted absorption of the sample is plotted for better comparison.

Figure 6. Time-resolved, laser-induced changes, $\Delta A(\lambda; t)$, in the absorbance of control chlorosomes under non-reducing conditions at two delays. The spectrum recorded at the longer delay has been multiplied by a constant in order to bring into coincidence the Car

TmS signal in the two spectra. The initial absorbance was 0.8 at 716 nm. The inverted absorption of chlorosomes is plotted for better comparison.

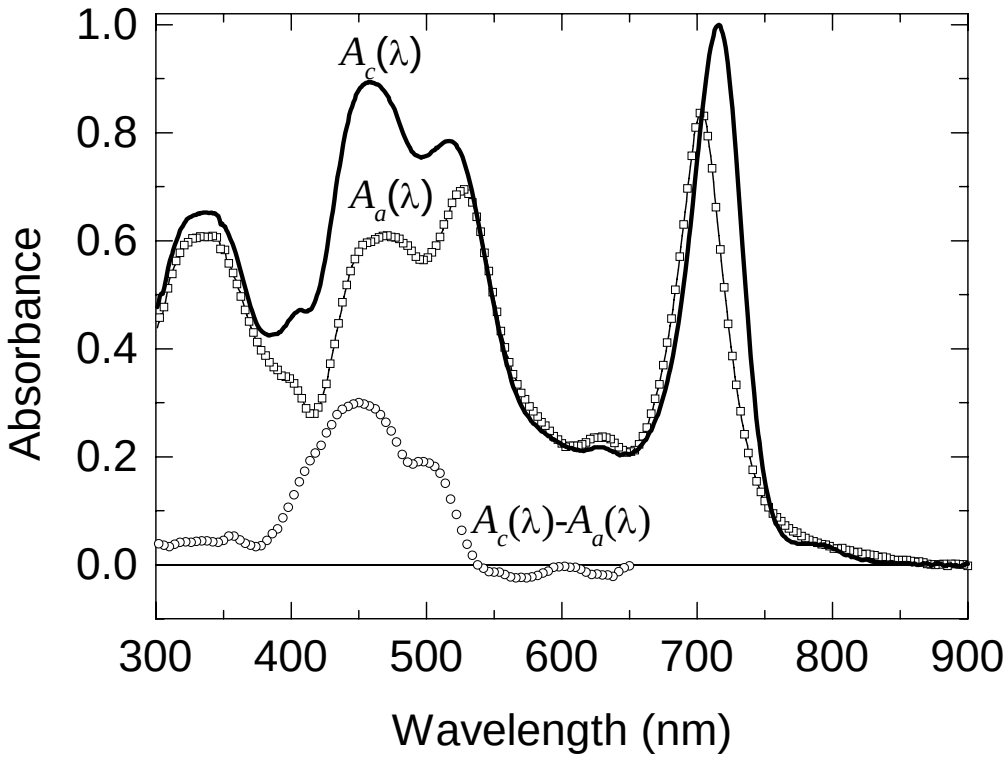
1.0
0.8
0.6
0.4
0.2
0.0
Absorbance
$A_c(\lambda)$
$A_a(\lambda)$
$A_c(\lambda)$-$A_a(\lambda)$
300
400
500
600
700
800
900
Wavelength (nm)

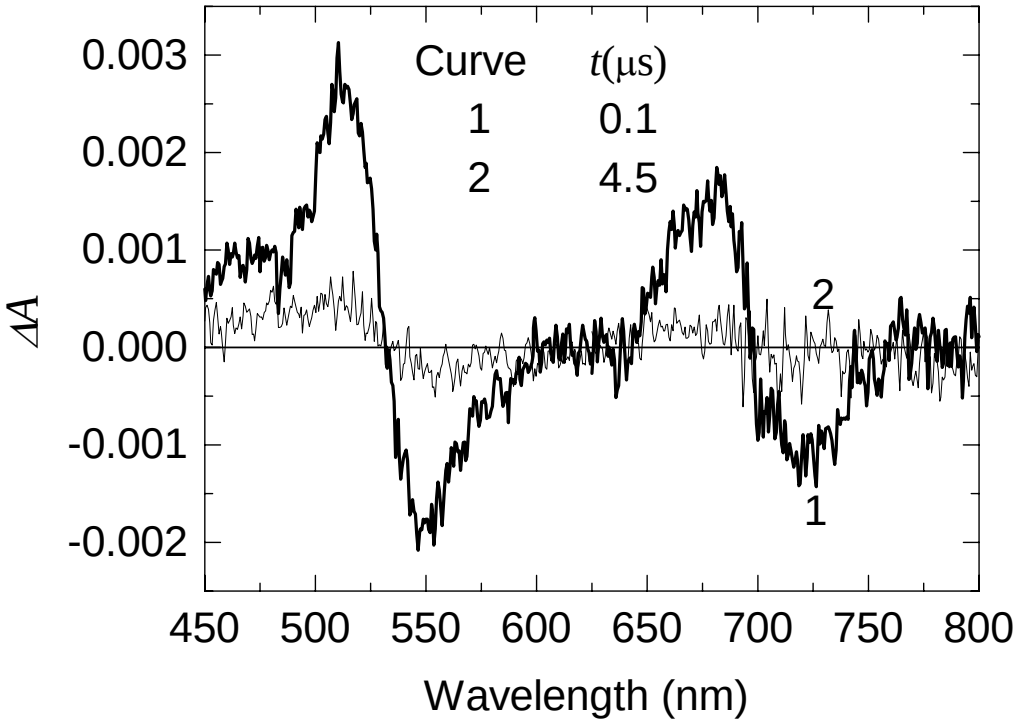
Curve
t(μs)
1
0.1
2
4.5
0.003
0.002
0.001
0.000
-0.001
-0.002
ΔA
2
1
450
500
550
600
650
700
750
800
Wavelength (nm)

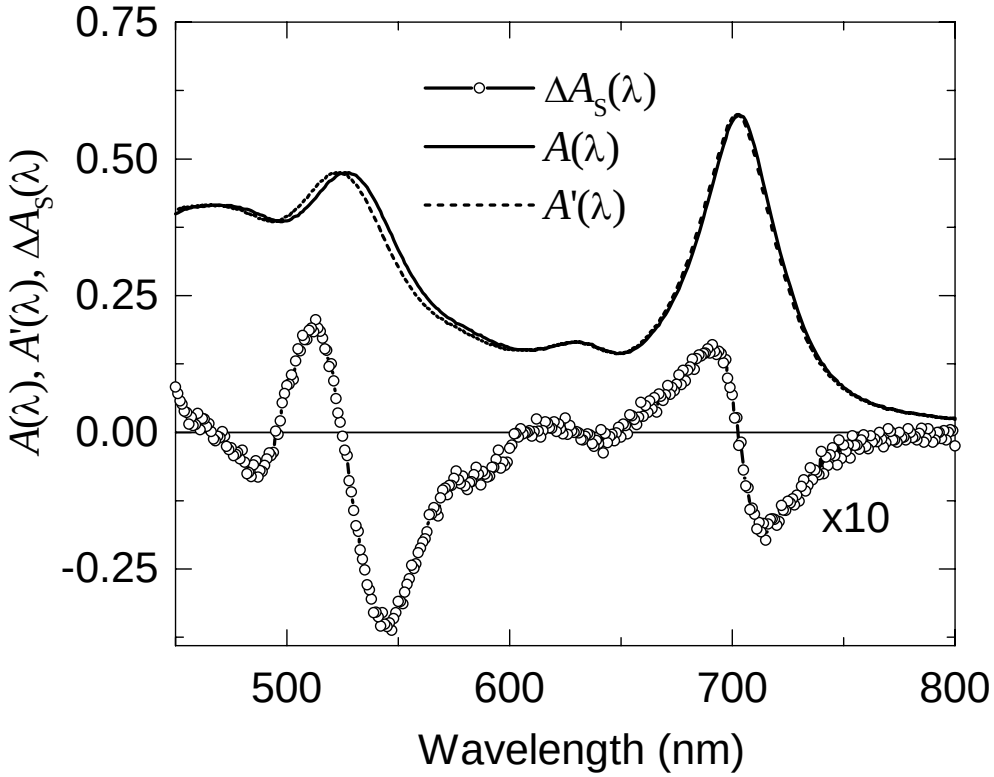
0.75
0.50
0.25
0.00
-0.25
$A(\lambda), A'(\lambda), \Delta A_S(\lambda)$
$\Delta A_S(\lambda)$
$A(\lambda)$
$A'(\lambda)$
x10
500
600
700
800
Wavelength (nm)

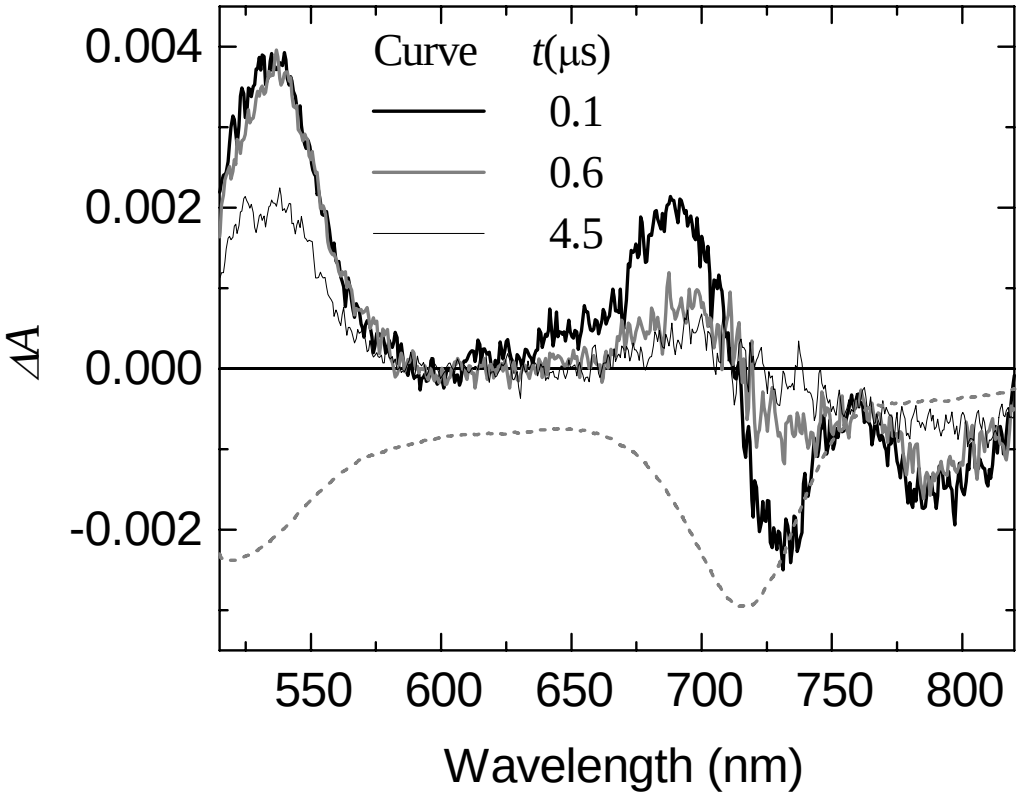
Curve
t(μs)
0.1
0.6
4.5
0.004
0.002
0.000
-0.002
ΔA
550
600
650
700
750
800
Wavelength (nm)

Figure 5

Arellano et al.

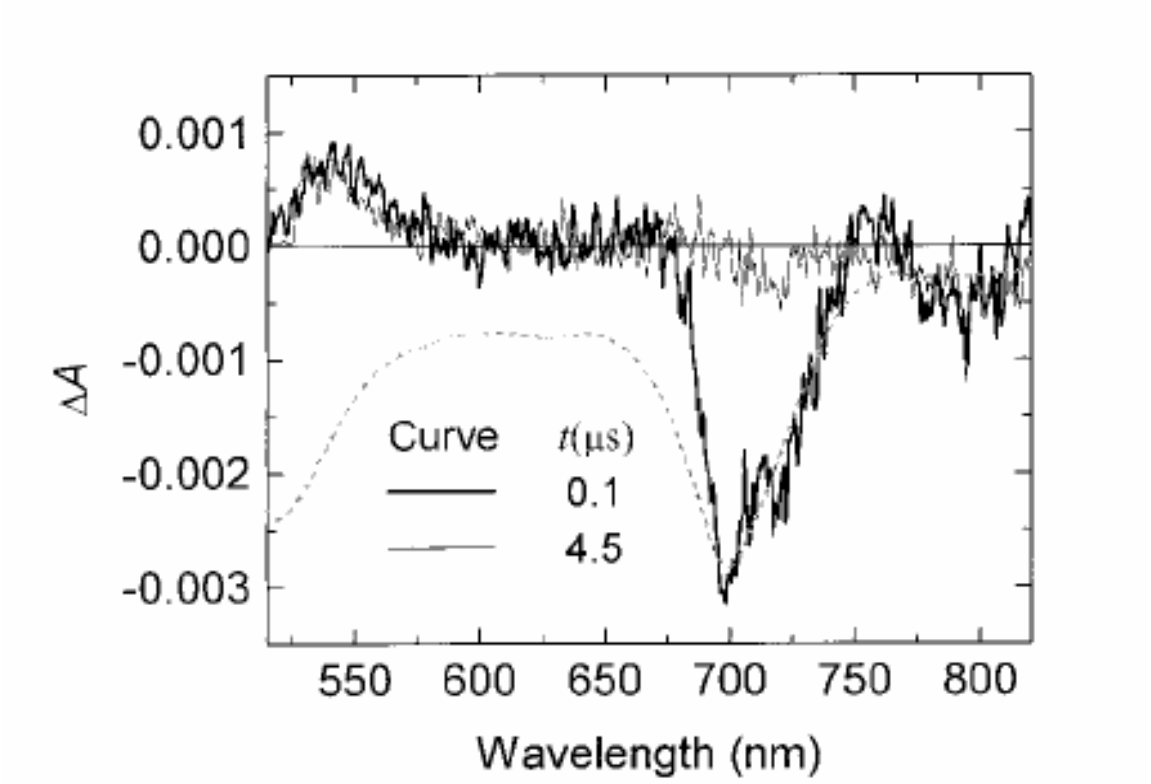

Figure 6

Arellano et al.